IEEE Access
Multidisciplinary ⋮ Rapid Review ⋮ Open Access Journal

Received May 12, 2020, accepted June 1, 2020, date of publication June 4, 2020, date of current version June 16, 2020.

Digital Object Identifier 10.1109/ACCESS.2020.3000044

Vein Biometric Recognition on a Smartphone

RAUL GARCIA-MARTIN AND RAUL SANCHEZ-REILLO, (Senior Member, IEEE)
Electronic Technology Department, University Carlos III of Madrid, 28911 Leganés, Spain
Corresponding author: Raul Garcia-Martin (raulgarc@ing.uc3m.es)

ABSTRACT Human recognition on smartphone devices for unlocking, online payment, and bank account verification is one of the significant uses of biometrics. The exponential development and integration of this technology have been established since the introduction in 2013 of the fingerprint mounted sensor in the Apple iPhone 5s by Apple Inc.© (Motorola© Atrix was previously launched in 2011). Nowadays, in the commercial world, the main biometric variants integrated into mobile devices are fingerprint, facial, iris, and voice. In 2019, LG© Electronics announced the first mobile exhibiting vascular biometric recognition, integrated using the palm vein modality: LG© G8 ThinQ (hand ID). In this work, in an attempt to become the become the first research-embedded approach to smartphone vein identification, a novel wrist vascular biometric recognition is designed, implemented, and tested on the Xiaomi© Pocophone F1 and the Xiaomi© Mi 8 devices. The near-infrared camera mounted for facial recognition on these devices accounts for the hardware employed. Two software algorithms, TGS-CVBR® and PIS-CVBR®, are designed and applied to a database generation and the identification task, respectively. The database, named UC3M-Contactless Version 2 (UC3M-CV2), consists of 2400 contactless infrared images from both wrists of 50 different subjects (25 females and 25 males, 100 individual wrists in total), collected in two separate sessions with different environmental light environmental light conditions. The vein biometric recognition, using PIS-CVBR®, is based on the SIFT®, SURF®, and ORB algorithms. The results, discussed according to the ISO/IEC 19795-1:2019 standard, are promising and pave the way for contactless real-time-processing wrist recognition on smartphone devices.

INDEX TERMS Vein biometric recognition, smartphone, wrist vascular biometric recognition, contactless database, biometrics on mobile devices, near-infrared camera, Xiaomi© Pocophone F1, Xiaomi© Mi 8, SIFT® (scale-invariant feature transform), SURF® (speeded up robust features).

I. INTRODUCTION

In recent years, biometric recognition has been a significant field in the security world that has witnessed an exponential increase in the integration of identification/authentication systems in daily life: access control, online payments, bank account access, and device unlocking. Security and, of course, comfort are the two leading causes. Hygiene is another important concern behind this constant and impressive growth of biometric-based systems, especially multi-user systems (e.g., access control). For this purpose, non-contact systems are designed. There are numerous contactless biometric modalities: facial, voice, iris, gait, vascular, and contactless fingerprint.

In previous research [1], paying attention to vascular recognition modality and the current patents of palm vein (Fujitsu© PalmSecure™, US 2005/0148876 A1 [2]) and finger vein (Hitachi© Finger Vein Authentication, US 2011/0222740 A1 [3]) variants, a portable contactless device for Vascular Biometric Recognition (VBR) was implemented and tested. In [4] and [5], other systems, with physical contact between the user and the device, were designed for wrist VBR. All these prototypes are suitable for access control and forensic applications. However, in the present work, a complete VBR system embedded into a smartphone, aimed for future online payments, bank account access, and screen unlocking, without touching the device, is proposed.

The associate editor coordinating the review of this manuscript and approving it for publication was Marina Gavrilova.

A. MOTIVATION

Smartphones are essential in daily life and are the systems with the most biometric modalities embedded simultaneously on the same device: fingerprint (e.g., Vivo© X20 [6]), facial (e.g., Huawei© Mate 20 Pro [7]), iris (e.g., Samsung© Galaxy S8 [8]) and voice (e.g., Google Assistant [9]).

This work is licensed under a Creative Commons Attribution 4.0 License. For more information, see https://creativecommons.org/licenses/by/4.0/

TABLE 1. Wrist VBR datasets.

Dataset	Subjects	Wrists	Samples	Sessions	Images	Year	Contactless
Singapore (NIR) [19]	150	2	3	N/A	900	2007	NO
UC3M [20]	121	1 (right)	5	1	605	2011	NO
PUT [18]	50	2	4	3	1200	2011	NO
Raghavendra et al. [4]	50	2	5	2	1000	2016	NO
UC3M-CV1 [1]	50	2	6	2	1200	2020	YES
UC3M-CV2 (Proposed)	**50**	**2**	**12**	**2**	**2400**	**2020**	**YES (smartphones)**

(a) (b)

FIGURE 1. Smartphones used for VBR integration (image capture, processing, and storage): Xiaomi© devices. (a) Xiaomi© Pocophone F1. (b) Xiaomi© Mi 8.

Likewise, in the research world, other modalities for smartphones are studied: gait [10], keystroke [11], or handwriting [12].

Last year, LG© Electronics company announced the first mobile with vascular biometric recognition integrated integrated using the palm vein modality: LG© G8 ThinQ (hand ID) [13]. This commercial launch, the high current integration of biometric systems into mobile devices, and the research approach in contactless recognition are the motivation behind this work.

B. CONTRIBUTIONS

In this study, a non-contact wrist vein biometric system integrated into a smartphone device is presented. For this purpose, two devices, designed by Xiaomi Inc.©, are used as complete capture, processing, and storage and storage hardware: Xiaomi© Pocophone F1 (Fig. 1 a) and Xiaomi© Mi 8 (Fig. 1 b). Both mobiles mount a near-infrared camera originally used to unlock them with facial recognition.

Two software algorithms have been proposed and registered: Three-Guideline Software for Contactless Vascular Biometric Recognition (TGS-CVBR®) and Pre-processing and Identification Software for Contactless Vascular Biometric Recognition (PIS-CVBR®). Both have been implemented using Android™. The former, TGS-CVBR®, has been used to generate a contactless database (UC3M-CV2), and it also provides feedback to the user on how to place the wrist correctly during the recognition process. Then, PIS-CVBR® is in charge of the biometric recognition task.

C. RELATED WORK

The current wrist VBR State-of-the-Art, in the research stage, has been recently analyzed in several works, [1] (published in the current year 2020) and [14], according to the existing systems, datasets, and algorithms. In addition, Tables 1 and 2 summarize the most recent literature showing, respectively, the existing databases and the recognition techniques, including their performance.

It is thought that there are no well-integrated and well-known commercial systems on the market based on the wrist vein modality. Also, as far as is known, published papers about vein systems integrated into a mobile phone do not exist. Only several works make use of smartphones but modifying their hardware: the infrared blocking filter is physically removed from the camera. These studies are based on the hand palm vein [15] and the hand dorsal vein [16] modalities.

The wrist VBR State-of-the-Art has been analyzed from the point of view of the recognition algorithms and techniques because the proposed acquisition hardware or system, a smartphone, is different and innovative. Furthermore, the absence of contact between the user and the capture system is a current stream of research that is starting to emerge, as is the case of [1] or [17] (finger vein modality).

According to Table 1, PUT [18] database, collected in 3 different sessions in 2014 with the participation of 50 subjects (50 subjects $\times$ 2 wrists $\times$ 4 samples $\times$ 3 sessions $=$ 1200 images), is the only existing public dataset. Two other privately-distributed databases were collected, respectively,

TABLE 2. State-of-the-Art summary for wrist VBR.

Study	Year	Dataset	Preprocessing	Feature Extraction	Feature Comparison/Classification	Computing time (seconds per sample)	Biometric performance
Das et al. [21]	2014	PUT	Monochromatic image + Adaptive histogram equalization + Discrete Meyer Wavelet	Dense Local Binary Pattern (D-LBP)	Support Vector Machines (SVMs)	0.771 (Windows®, Matlab®, Intel® i5 CPU)	EER = 0.79 %
Raghavendra et al. [4]	2016	Raghavendra et al. [4]	Monochromatic image + Contrast Limited Adaptive Histogram Equalization (CLAHE)	Local features: Maximum Curvature Points (MCP) and Multi-scale match filter. Global features: Sparse Representation Classifier (SRC), Local Binary Patterns (LBP), Local Phase Quantization (LPQ), Histogram of Gradients (HOG), Steerable pyramids, Local Binary Patterns Variance (LBPV) and Log Gabor Filters	Local features: Cross-correlation. Global features: Sparse Representation Classifier (SRC)	N/A	EER = 1.63 %
Mohamed et al. [14]	2018	PUT	Monochromatic image + Median filter + CLAHE	Binarization (local and global threshold)	Maximum value 2D correlation + Score fusion with Parade t-norm	N/A	EER = 0.0 %
Nikisins et al. [22]	2018	PUT	Monochromatic images + Gaussian filter + k-means++ algorithm + Region Of Interest (ROI) extraction	Hessian matrix	Cross-correlation based comparison	0.92 (Linux™, Python™, Intel® i7-5930K CPU)	FNMR = 3.75 % & FMR = 0.1 %
Proposed	**2020**	**UC3M-CV2**	**Monochromatic image + CLAHE + Gaussian, median and averaging filters (11 x 11)**	**SIFT®, SURF® and ORB**	**Brute Force Matching (BFM) and Fast Library for Approximate Nearest Neighbors (FLANN)**	**0.317 (Qualcomm® Snapdragon™ 845: Octa-Core and 2.8 GHz)**	**EER (Pocophone F1 smartphone)= 14.76 %**

in 2007 and 2011, and have been used in other research works in later years: Singapore [19] and UC3M [20]. Also, other studies use their private dataset, as is the case of [1] and [4]. As far is known, the UC3M-CV1 [1], along with the database collected in this work, UC3M-CV2, is the only one that includes contactless image acquisition. UCM3-CV2 presents the most extensive dataset, with 2400 images, although the 50 subjects are far from the 150 of the Singapore database.

The recognition software algorithms have been classified into three groups or steps: preprocessing, feature extraction, and feature comparison or classification. The absence of Deep Learning techniques applied to the wrist VBR modality is the cause of this traditional recognition division. However, some examples of Deep Learning research are referenced further on for the finger vein variant.

The most common preprocessing or intermediate biometric sample processing techniques, starting from monochromatic infrared images, are histogram equalization ([4], [14], and [21]), and noise reduction using filters (2D Median and Gaussian filters, [14] and [22]). These steps are followed to isolate and enhance the visualization of the patterns described by the vascular tissues.

Then, for feature extraction, several techniques have been used: Dense Local Binary Pattern (D-LBP) in [21]; Maximum Curvature Points (MCP), Multi-scale match filter, Sparse Representation Classifier (SRC), LBP, Local Phase Quantization (LPQ), Histogram of Gradients (HOG), Steerable pyramids, Local Binary Patterns Variance (LBPV), and Log Gabor Filters in [4]; Binarization in [14] and Hessian matrix in [22]. Most of these methods, based on segmentation and

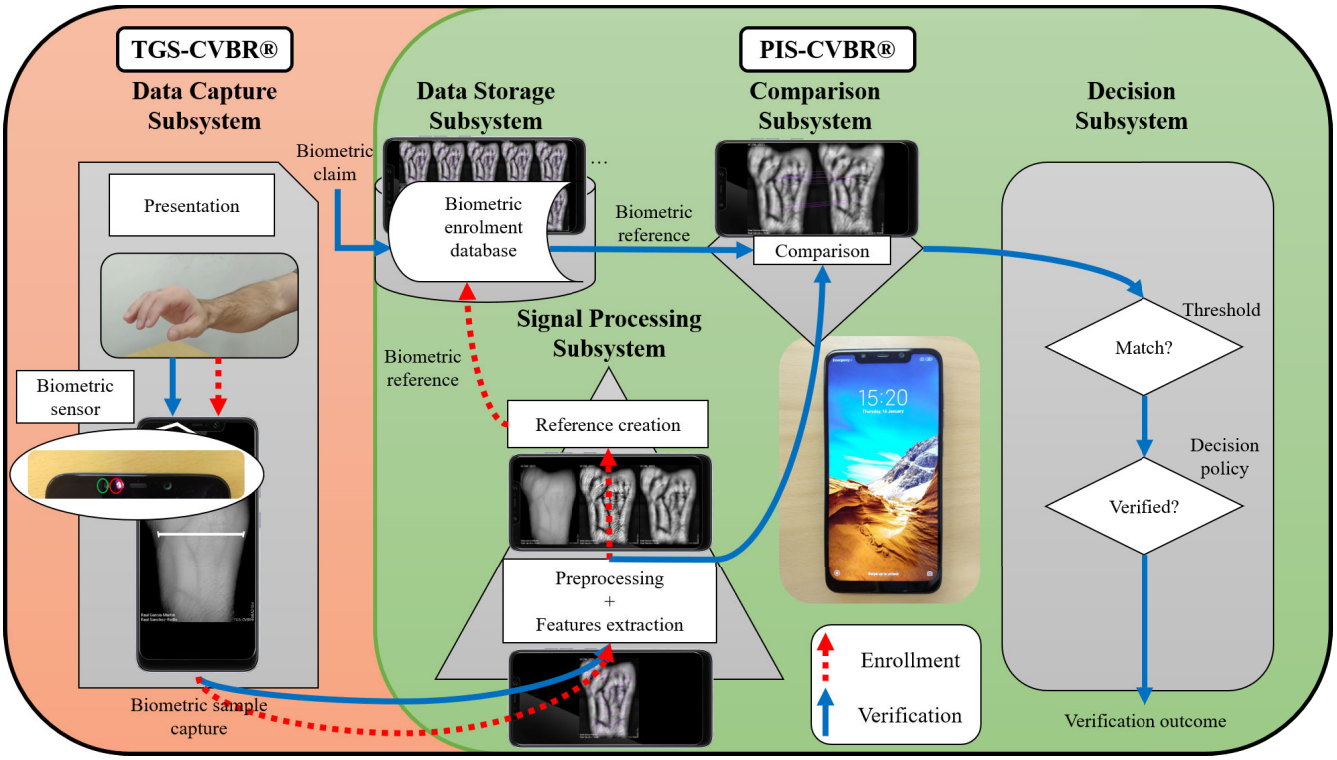

FIGURE 2. Components of the designed VBR system embedded on a Smartphone.

biometric template comparison, are not robust enough against vein tissue orientation, scale, or even deformation [23].

In this sense, as Matsuda *et al.* [23] claim, minutiae-based techniques (e.g., [20], not in Table 2) and SIFT methods are usually more robust. In the proposed study, to avoid the scale and orientation variability, in the vein patterns, due to the non-contact acquisition that does not fix the wrist position, the algorithms SIFT®, SURF®, and ORB have been tested and applied. In addition, a contactless guiding algorithm, TGS-CVBR®, has been designed to lead the user through wrist positioning and reduce the scale and orientation variations. SIFT®, SURF®, and ORB are local feature extractors for homography based on the image intensity variability described by corners and edges (Harris Corner Detector [24]).

Traditional Machine Learning techniques for feature comparison/classification were introduced in [21] with the supervised technique Support Vector Machines (SVMs). In the current work, other supervised Machine Learning method, based on k-Nearest Neighbor (kNN), has been used for the SIFT® and SURF® keypoints classification: Fast Library for Approximate Nearest Neighbor (FLANN). Another remarkable procedure, presented in [14], was exhibited in 2018 with the biometric score fusion of both subjects' wrists. This work states the best biometric performance, without considering the database figures and external conditions (e.g., contact and external light isolation). The computational cost, not indicated in some works (N/A), is also provided in Table 2.

As has been mentioned previously, Deep Learning has not been applied to wrist VBR modality. However, essential advances in the use of Convolutional Neural Networks (CNNs) have already been stated in other vascular modalities, like finger vein variant. The CNN architecture, used in [25], where a complete finger vein State-of-the-Art is presented, achieves an identification accuracy greater than 95 % in several databases. For the same VBR modality, a CNN architecture comparison and analysis (AlexNet, VGGNet, and ResNet) is exposed in [26] obtaining a DenseNet CNN with EER values less than 1 %. On the other hand, reference [23] provides an EER lower than 1 % using a non-Deep Learning method based on deformation-tolerant features against vein deformations (different finger postures).

For a complete VBR analysis, reference [27] is highly recommended.

In order to contribute to ongoing research and provide the possibility of realizing an even stricter comparison of the software techniques according to existing datasets, a Python™ version of the proposed software algorithms has been published [28] (https://joinup.ec.europa.eu/solution/vein-biometric-recognition-smartphone) under the terms and conditions of the Creative Commons Attribution Non-Commercial license (CC-BY-NC-SA-4.0).

II. DESIGNED SYSTEM

Following the standard ISO/IEC 19795-1:2019 [29], the system has been designed according to the scheme in Fig. 2. As this figure shows, the recognition process starts with the

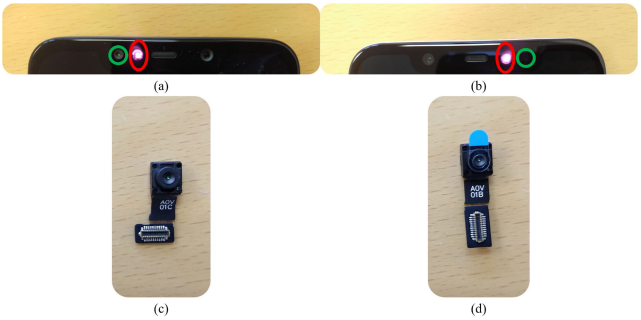

FIGURE 3. Capture hardware: (a) Xiaomi© Pocophone F1 near-infrared camera (surrounded in green) and near-infrared LED near-infrared LED (surrounded in red) embedded on the left side of the notch. (b) Xiaomi© Mi 8 near-infrared camera (surrounded in green) and near-infrared LED (surrounded in red) on the right side of the notch. (c) Xiaomi© Pocophone F1 near-infrared camera (non-mounted replacement). (d) Xiaomi© Mi 8 near-infrared camera (non-mounted replacement).

acquisition of the user's sample through the biometric sensor of the smartphone: a near-infrared camera. The capture and guiding algorithm, TGS-CVBR®, is in charge of this task. Then, the captured image is processed in two steps (signal processing subsystem) through PIS-CVBR®: preprocessing and feature extraction. The unique features extracted are stored in a database and compared to identify or verify the user.

A. INTEGRATED BIOMETRIC HARDWARE

In order to obtain a real-time wrist VBR system, all the software tasks (database collection, database storage, image preprocessing, feature extraction, and feature comparison) are processed in the same hardware: a smartphone. Two mobile devices, designed by the Chinese company Xiaomi Inc.© have been selected and used used independently: Xiaomi© Pocophone F1 (Fig. 1 a) and Xiaomi© Mi 8 (Fig. 1 b). The main reason for using these models is the embedded near-infrared camera for facial recognition, only available in a few commercial smartphones. The near-infrared cameras and the near-infrared LED (Light Emitting LED (Light Emitting Diode) lights emitted by the mobile phones, required for VBR, are shown in Fig. 3 a, b, and Fig. 3 c, d (replacement cameras not mounted).

The details about the components, camera and LED, and their features are unknown due to the commercial protection. It has only been possible to buy non-mounted replacement cameras and to verify that the LED light flashes at 30 Hz (measured with Thorlabs© PDA10CF-EC InGaAs Amplified Detector) and has a wide spectrum around 960 nm (measured with Yokogawa© AQ6370B Optical Spectrum Analyzer). It is essential to point out that no hardware modifications have been made. The main relevant hardware features of these two devices are summarized in Table 3.

B. SOFTWARE ALGORITHMS

The recognition algorithm presented in this paper is divided into two software algorithms: TGS-CVBR®, employed to guide users on how to place the wrist in the identification process and the database collection (image capture and visualization on the smartphone screen) and PIS-CVBR®, in charge of the recognition tasks.

TABLE 3. Relevant hardware features for Xiaomi© Pocophone F1 [30] and Xiaomi© Mi 8 [31].

	Feature	Xiaomi© Pocophone F1	Xiaomi© Mi 8
Hardware	Infrared Face Recognition Camera	Unknown (640 × 480 greyscale images)	Unknown (640 × 480 greyscale images)
	CPU	Qualcomm® Snapdragon™ 845 (Octa-Core, 2.8 GHz)	Qualcomm® Snapdragon™ 845 (Octa-Core, 2.8 GHz)
	GPU	Qualcomm® Adreno™ 630, up to 710 MHz (710 MHz)	Qualcomm® Adreno™ 630, up to 710 MHz (710 MHz)
	RAM	6 GB	6 GB
	Internal Storage	64 GB	64 GB
	Screen	IPS LCD full-screen 6.18" (1080 × 2246 pixels)	AMOLED full-screen 6.21" (1080 × 2248 pixels)
	Size	155.5 × 75.2 × 8.8 mm	154.9 × 74.8 × 7.6 mm
	Weight	182 g	175 g
Software	OS	Android™ 9 Pie	Android™ 9 Pie
	MIUI Version	Global 10.2	Global 10.1

1) TGS-CVBR®

This software algorithm displays the real-time video of the near-infrared camera capture (640 × 480 resolution) on the smartphone screen and three fixed guidelines, as it is shown in Fig. 4. It provides feedback to the user on how to place the wrist correctly. Also, it has been used for database generation (UC3M-CV2 database) and user identification, combined with PIS-CVBR®. It fixes the user's wrist, obtaining scale-orientation-invariant images to improve the identification process. The horizontal guideline sets the wrist orientation, and the two smaller guidelines establish the distance between the wrist and the smartphone camera.

The user should follow the steps shown in Fig. 4 a:

1) Locate the wrist groove print or mark.
2) Align/match the wrist groove print with the guide trace displayed.

This software has been developed using Android™ and has been run in Android™ 9 Pie OS version (MIUI© Global

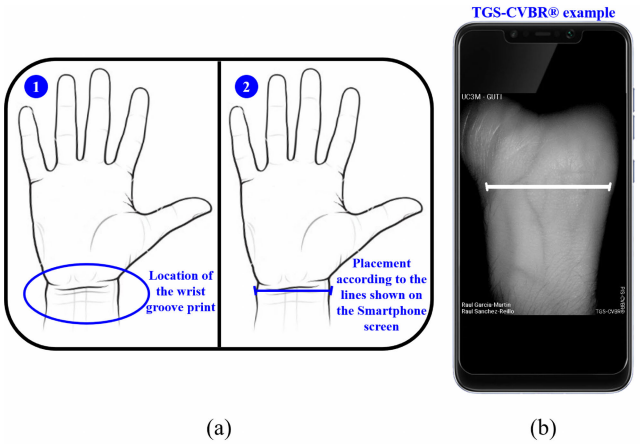

FIGURE 4. TGS-CVBR® (Three-Guideline Software for Contactless Vascular Biometric Recognition), wrist positioning steps. (a) Step 1: location of the wrist groove line. Step 2: match of the wrist groove print and the guideline. (b) TGS-CVBR® example on Xiaomi© Pocophone F1.

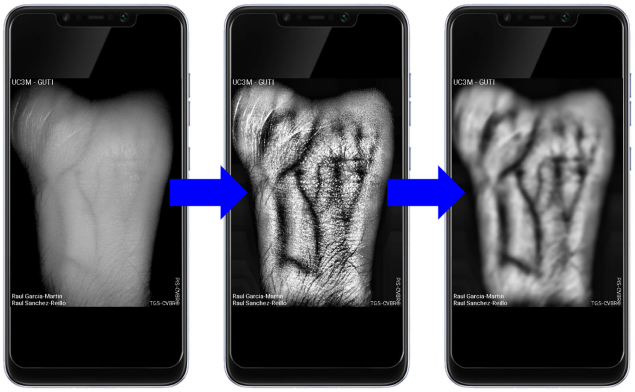

FIGURE 5. PIS-CVBR®: Preprocessing. Steps in a User 0 sample (images from Xiaomi© Pocophone F1): (a) Greyscale image. (b) Image after CLAHE algorithm. (c) Image after CLAHE algorithm and filtered by Gaussian filter, Median filter, and Averaging (11 × 11 kernel).

Global 10.2 in Xiaomi© Pocophone F1 and MIUI© Global 10.1 in Xiaomi© Mi 8). It is essential to point out that, access the near-infrared camera, the devices have been rooted, obtaining superuser permissions.

2) PIS-CVBR®

The Preprocessing and Identification Software for Contactless Vascular Biometric Recognition (PIS-CVBR®) proposed is divided into three parts: preprocessing, feature extraction, and feature comparison.

1) Preprocessing:
For each device, the near-infrared camera provides greyscale images (monochromatic images with values from 0, black, to 255, white) with 640 × 480 resolution. The images have been captured in ''.jpg'' compress format (Fig. 5 a, User 0's sample of the dataset) using TGS-CVBR®, the near-infrared camera, and the near-infrared LED.

To increase the contrast between the veins and the other living tissue, the adaptative histogram equalization technique, CLAHE (Contrast Limited Adaptive Histogram Equalization) [32], has been applied (Fig. 5b). To reduce the high-frequency noise (salt-and-pepper and Gaussian noise) generated by the CLAHE algorithm, several low-pass software filters have been applied (Fig. 5 c) in the following order: Gaussian filter, Median filter, and Averaging filter. The kernel size of all of them is 11 × 11.

No further steps have been taken for the preprocessing task. It is essential to remark that the Region Of Interest (ROI) extraction has not been required by this software algorithm, due to the excellent isolation from the background obtained with the cameras, with a short distance design and LED lights emitted by the smartphones. However, it would probably improve system performance and is a step to take into account in the future.

2) Feature Extraction:
In order to deal with the complexity of the biometric recognition task, due to the non-physical-contact property of the proposed solution, three scale-orientation-invariant algorithms for homography have been tested for the extraction of unique features from the wrist vein patterns: SIFT® (Scale-Invariant Feature Transform) [33], SURF® (Speeded Up Robust Features) [34] and ORB (Oriented FAST and Rotated BRIEF) [35]. The main reason to use these algorithms is the high variability observed in the size and orientation of the wrist in each user sample when the system is contactless. As was mentioned, and it is shown in the experiment and result section (Section III), the proposed TGS-CVBR® algorithm solves this issue. In the VBR world, as far as is known, these three algorithms, SIFT®, SURF®, and ORB, have been tested in [1] and only SIFT® in [36].

SIFT®, the non-free patent algorithm, was proposed in [33] to avoid the scale variant of the Harris Corner Detector [24] features. Then, SURF® [34] was presented as a real-time solution due to the slow feature extraction process of SIFT®. Finally, ORB [35], even faster, is a free use solution for the feature extraction (key points and its descriptors). To obtain a real-time contactless system embedded into a smartphone these three feature extraction algorithms have been tested and compared, considering its evolution and processing time.

Fig. 6 a, b, and c show, respectively, one example of feature extraction, 100 key points, for each algorithm. The location, scale, and orientation of the features are represented. As can be observed, especially for SIFT® and SURF® key points, the descriptors are homogeneously distributed throughout the vein lines and the surrounded tissue. Probably, this fact increases the robustness of the proposed algorithm, not only

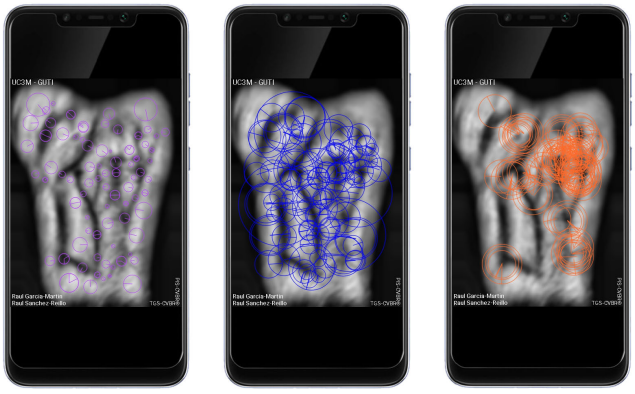

(a) (b) (c)

FIGURE 6. PIS-CVBR®: Feature extraction. Scale and orientation of 100 key points extracted from a User 0 sample with the three algorithms: (a) SIFT®. (b) SURF®. (c) ORB.

considering vein patterns but also the surrounded areas influenced by them. In future work, a more extreme segmentation (e.g., binarization + skeletonization) could be compared with the proposed solution to verify this hypothesis.

3) Feature Comparison:
Following the feature extraction algorithms used, the optimum comparison algorithms selected and applied have been Brute Force Matching (BFM) and Fast Library for Approximate Nearest Neighbors (FLANN) [37]. BFM, implemented for the ORB features, and FLANN, used for the SIFT® and SURF® features, provide similarity distance values between the descriptors of the key points extracted. As was mentioned in the introduction, FLANN is a supervised classification Machine Learning technique based on k-Nearest Neighbor (kNN). In the BFM case, the Hamming distance has been used.
Fig. 7 a, b, and c show, respectively, an example of feature comparison for the three feature extraction algorithms, SIFT®, SURF® and ORB, and the two comparison processes, BFM and FLANN.
This software algorithm has been also developed using Android™ and has been run in Android™ 9 Pie OS version (MIUI© Global 10.2 in Xiaomi© Pocophone F1 and MIUI© Global 10.1 in Xiaomi© Mi 8).

3) TGS-CVBR® AND PIS-CVBR® COMBINED: DECISION POLICY

With the main goal of obtaining a real-time authentication and identification system, taking into account the computing time, TGS-CVBR® and PIS-CVBR® have been combined and tested.

To decide if the matched points are suitable (distance small enough), after the feature comparison of the PIS-CVBR® algorithm, a distance score threshold has been implemented,

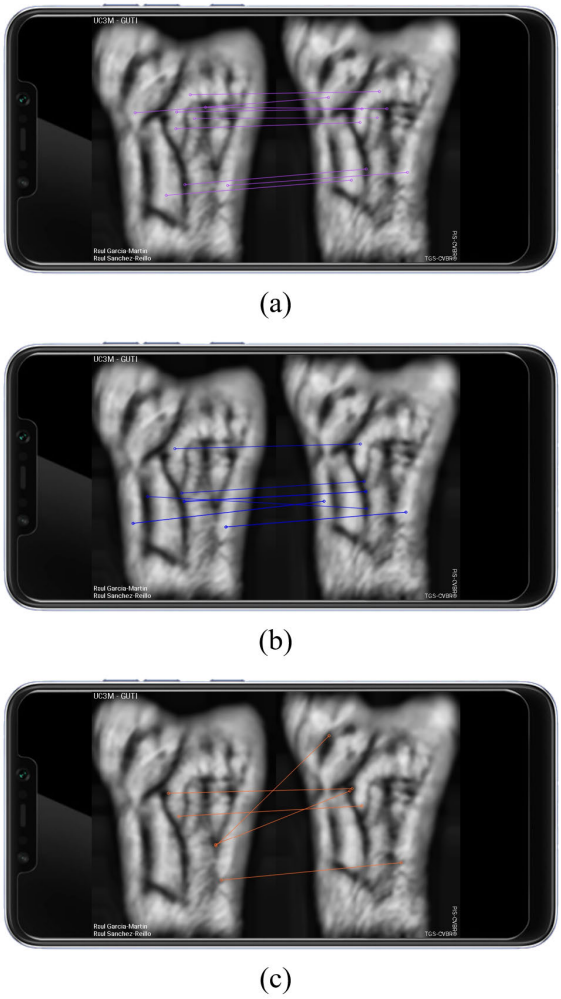

(a) (b) (c)

FIGURE 7. PIS-CVBR®: Feature comparison. Correct matching points for two samples of the User 0 with the three feature extraction algorithms and the two comparison algorithms: (a) SIFT® (with FLANN). (b) SURF® (with FLANN). (c) ORB (with BFM).

following

$$Match_{BFM} = \begin{cases} Correct, & \text{if } d < \delta \\ Incorrect, & \text{if } d \geq \delta \end{cases} \quad (1)$$

where:

- d: is the comparison distance.
- δ: is the selected distance threshold.

FLANN, used for the SIFT® and SURF® descriptors, also provides similarity distances. In this case, the matches are filtered with the Lowe's ratio, as in

$$Match_{FLANN} = \begin{cases} Correct, & \text{if } d \times R < \delta \\ Incorrect, & \text{if } d \times R \geq \delta \end{cases} \quad (2)$$

where:

- d: is the comparison distance.
- R: is the Lowe's ratio.
- δ: is the selected distance threshold.

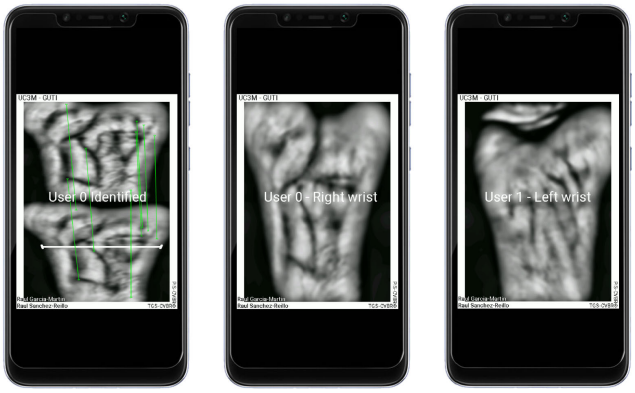

FIGURE 8. TGS-CVBR® and PIS-CVBR® combined (decision policy): captures of the verification and identification process for the SIFT® algorithm and Lowe's ratio filtering. (a) Verification of the User 0 (subject 0, right wrist). (b) Identification of the User 0 (subject 0, right wrist). (b) Identification of the User 1 (subject 0, left wrist).

For the authentication/verification process (1:1 user comparison), the features extracted from the previously defined user vein pattern are compared with the real-time video capture, i.e., the key points from the pattern (Fig. 8 a, top) are compared with the key points obtained from the video (Fig. 8 a, bottom). This process is shown on the screen of the devices.

In the identification process (1:N user comparison), the key points of the real-time video capture are compared with the ones previously obtained and defined from the users' patterns. Fig. 8 b and c show an example of the User 0 identification. It is essential to remark that according to the standard ISO/IEC 19795-1:2019 [29], this software algorithm combination does not identify because it does not provide a rank of potential candidates.

C. DATABASE

The contactless dataset generated to test the system is named UC3M-CV2 database (UC3M-Contactless Version 2). It has been collected with TGS-CVBR®, PIS-CVBR®, and both smartphones.

1) PARAMETERS

1) Subject conditions:
The UC3M-CV2 database consists of 2400 near-infrared greyscale 640 × 480 images captured from 100 users: both wrist of 50 subjects (25 females and 25 males) from Europe (43), America (4), Africa (1) and Asia (2) aged between 21 and 75 years (39.92 years on average, 17.74 standard deviation). The age-origin distribution is shown in Fig. 9.
Two capture sessions, separated between 2 and 4 weeks, have been performed. Per each mobile device, Pocophone F1 and Mi 8, and subject wrist, six samples per session have been taken: 50 *subjects* × 2 *wrists* × 6 *samples* × 2 *sessions* × 2 *devices* = 2400 *images*. These images have been stored in the internal memory of the devices in ".jpg" compress format.

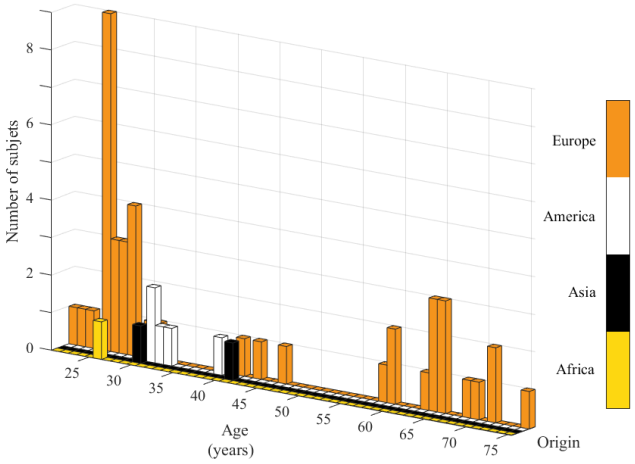

FIGURE 9. UC3M-CV2 database: distribution of the 50 subjects by age and origin.

2) Environmental conditions:
The samples have been taken under the following conditions:

a) *Temperature: approximately 20-23 °C.*
b) *Humidity: dry ambient.*
c) *External light: different daytimes, places (outdoor/indoor), and external artificial or natural light (usually without direct sunlight).*

2) COLLECTION METHOD

The next steps have been followed for the UC3M-CV2 collection:

1) The volunteers are informed of the experiment they will be part of and their rights according to the last General Data Protection Regulation (GDPR, applied since May 25th, 2018) [38]. Then, they sign the explicit consent.
2) Registration of the personal data of the subject.
3) Brief demonstration of the process to be followed, as it is shown in Fig. 4, to position the wrist correctly according to TGS-CVBR®.
4) An operator takes one capture when the user's wrist is placed correctly advising the user (voice indications) if the wrist is placed in an extremely wrong way: too far/near from the camera (not taking into account the two small guidelines) or with an incorrect orientation (not placing the wrist grove print aligned with the largest guideline).
5) The capture process is repeated, obtaining 24 samples per each subject (6 samples per wrist and 2 devices): one session per subject. The capture order for the devices has been Mi 8-Pocophone F1 in Session 1 and Pocophone F1-Mi 8 in session 2. The external light conditions between the different subjects are not the same: different days at a different time in different places (outdoor/indoor).

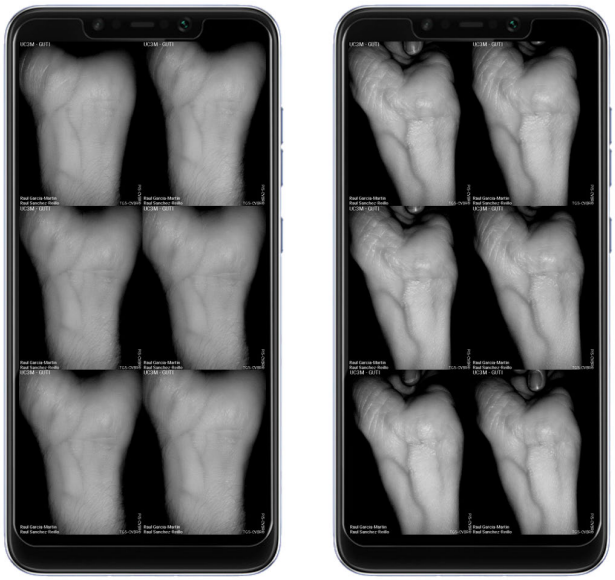

(a) (b)

FIGURE 10. TGS-CVBR® results: similar scale-orientation wrist images. (a) Six samples obtained from the User 0. (b) Six samples obtained from the User 82.

6) Between two and four weeks after the first session, steps 4 and 5 are repeated in the second session obtaining 48 samples per each subject (24 samples per wrist) in total.

III. EXPERIMENTS AND RESULTS

To obtain the biometric and the computing time performance of the proposed system, the software algorithms presented in this work, TGS-CVBR® and PIS-CVBR®, have been faced with the 2400-images dataset collected. The evaluation of them has been divided. However, the biometric performance is very closely correlated to the union of both algorithms.

A. TGS-CVBR

To study this algorithm, the dataset, UC3M-CV2, has been visually analyzed. Fig. 10 shows the results: 6 samples of the User 0 and User 82 of the database. As can be extracted from these images, using the contactless guiding algorithm, the size or scale, and the orientation of the wrist of each user are the same. In consequence, the illumination of the wrist area is homogeneous and is stabilized for every sample. These facts simplify the recognition task.

The distance between the near-infrared camera of the smartphones and the user's wrist has been usually 7-10 cm, depending on the width of each user's wrist.

B. PIS-CVBR

The analysis of this algorithm has been divided into two experiments or tests: biometric performance and computing-time performance

1) BIOMETRIC PERFORMANCE

Following the current standard ISO/IEC 19795-1:2019 [29], the results have been obtained and exposed according to the three feature extraction algorithms, SIFT®, SURF®, and ORB, and the two devices used, Pocophone F1 and Mi 8.

As is mandatory by the standard [29], the False Match Rate (FMR) and False Non-Match Rate (FNMR) are provided in a Detection Error Trade-Off (DET) plot (recommended). Failure-To-Enrol Rate (FTER) and Failure-To-Acquire Rate (FTAR) are zero.

DET curves have been obtained comparing, with FLANN (SIFT® and SURF® features) and BFM (ORB features), the 1200 images (Sessions 1 and 2) of each device, separately: 1100 intraclass or mated comparisons (50 *subjects* × 2 *wrist patterns* × 11 *samples*) and 108900 interclass or non-mated comparisons (100 *wrist patterns* × 99 *wrist patterns* × 11 *samples*). Fig. 11 shows the DET curves for Pocophone F1 (a, b, and c) and Mi 8 (d, e, and f) devices, the algorithms, SIFT® (a and d), SURF® (b and e), and ORB (c and f), and the different sessions (Session 1, Session 2 and both together).

Analyzing the variability in all the DET curves according to the sessions, the best performance has been obtained for Session 2, most probably, due to the better interaction and practice acquired by the subject placing the wrist using the designed guiding algorithm. The curves are closer to small values (lower FNMR and FMR) for Session 2 than for Session 1 and both sessions together, regardless of the feature extraction and comparison algorithm and the devices.

The different behavior observed in the curves comparing the results for the 1200 images of each smartphone, Pocophone F1 (Fig. 11 a, b, and c) and Mi 8 (Fig. 11 d, e, and f), could be considered negligible. The curves illustrate that the Pocophone F1 presents a slightly better performance. It is probably due to the positioning practice acquired by the subject in the sessions (previously cited) and not to the hardware performance. The images have been taken firstly with the Mi 8 and secondly with the Pocophone F1 in Session 1 and vice versa in Session 2 (the influence of the positioning practice in the sessions seems to be higher than the order of the devices in the database collection). In addition, it is thought that the near-infrared camera sensor and the near-infrared LED for both smartphones are very similar.

Finally, analyzing Fig. 11, all the curves indicate that the SIFT® feature extraction algorithm (FLANN feature comparison) provides the best performance (EER = 14.76 % for the full dataset of the Pocophone F1 device and EER = 17.03 % for the full dataset of the Mi 8 device).

Although the Equal Error Rate (EER) analysis is deprecated according to the standard [29], the assertions previously discussed could be summarized in Fig. 12.

The EER, for the three features extraction algorithms, is given over the different sessions of the datasets (Pocophone F1 dataset, Mi 8 dataset, and the full UC3M-CV2 dataset with

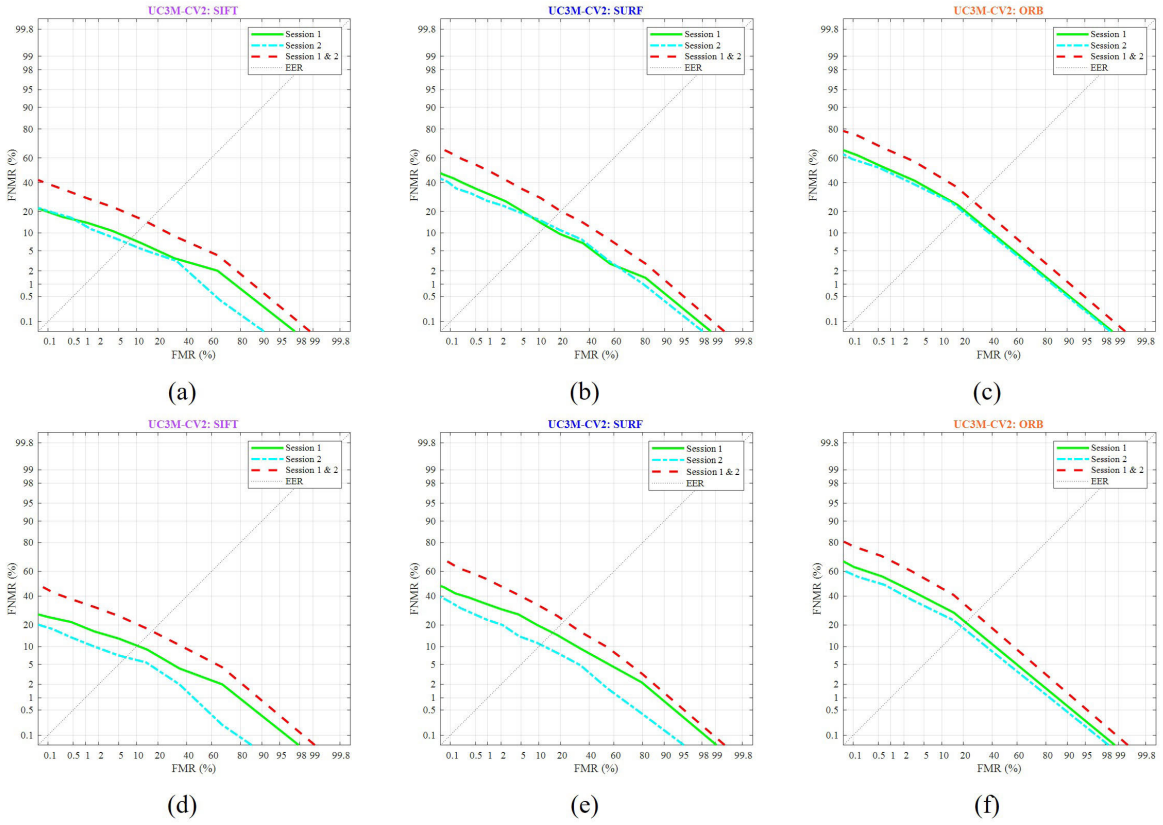

FIGURE 11. Biometric performance: DET curves. The FNMR (False Non-Match Rate) is represented versus the FMR (False Match Rate). The green (continuous), cyan (line-dot), and red (line-line) curves are respectively for Session 1, Session 2, and Session 1 & 2. (a) Xiaomi© Pocophone F1 with SIFT®. (b) Xiaomi© Pocophone F1 with SURF®. (c) Xiaomi© Pocophone F1 with ORB. (d) Xiaomi© Mi 8 with SIFT®. (e) Xiaomi© Mi 8 with SURF®. (f) Xiaomi© Mi 8 with ORB.

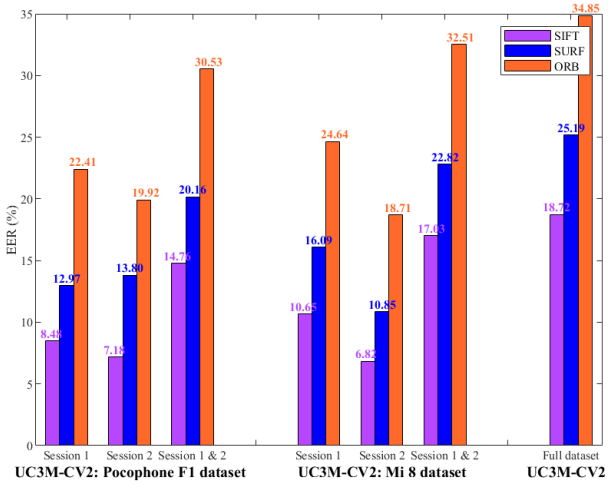

FIGURE 12. Biometric performance: EER for the Pocophone F1 dataset (1200 images, 1100 genuine comparisons, and 108900 impostor comparisons), Mi 8 dataset (1200 images, 1100 genuine comparisons, and 108900 impostor comparisons) and full UC3M-CV2 dataset (2400 images, 2300 genuine comparisons, and 227700 impostor comparisons).

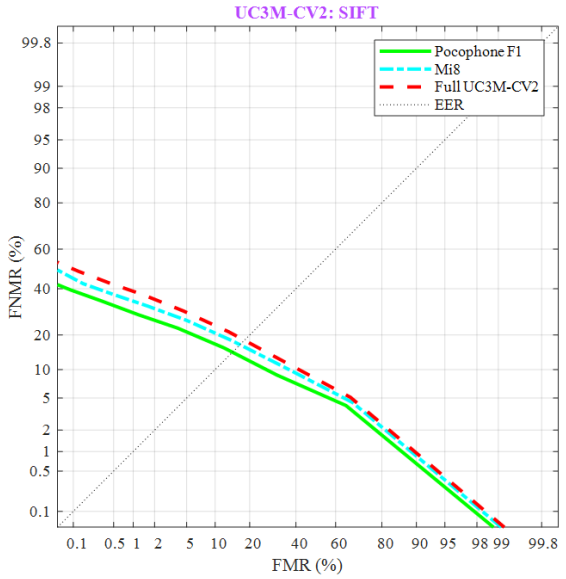

FIGURE 13. Biometric performance: DET curves for the SIFT® algorithm (FLANN comparison) using the Pocophone F1 dataset (continuous green curve), the Mi 8 dataset (line-dot cyan curve), and the full UC3M-CV2 dataset (line-line red curve).

2400 images, 2300 genuine comparisons, and 227700 impostor comparisons).

To conclude the biometric performance, Fig. 13 shows the DET curve of the selected algorithm, SIFT®, for the Pocophone F1 dataset (1200 images), the Mi 8 dataset (1200 images), and both datasets (2400 images).

These results have been obtained using Matlab® R2019b.

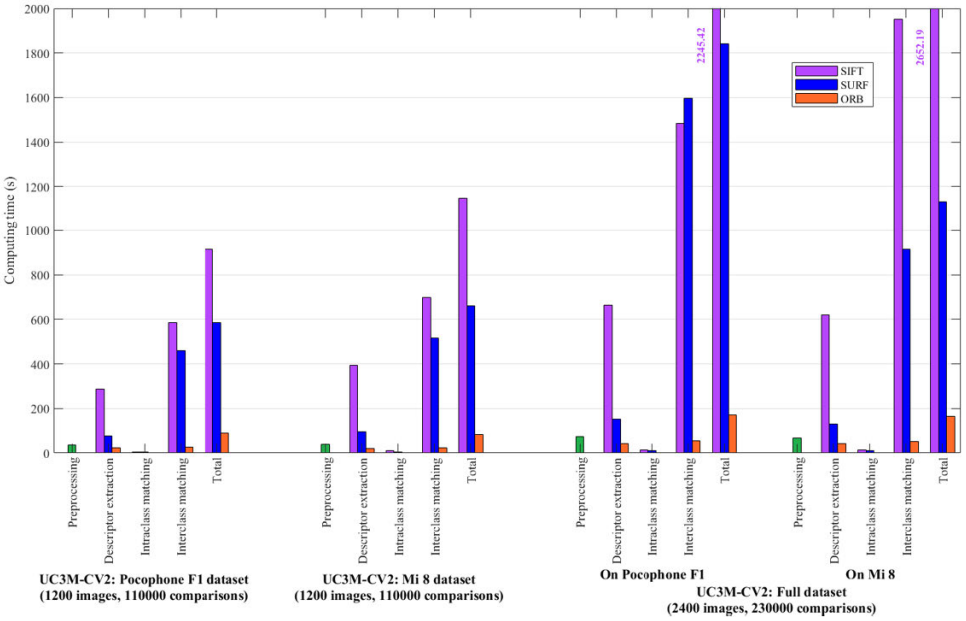

FIGURE 14. Computing time performance: time invested for the different algorithms (SIFT® SURF® and ORB), processes, and datasets run on the devices.

TABLE 4. Unit processing time (two samples comparison).

Task		Xiaomi© Pocophone F1 (ms)	Xiaomi© Mi 8 (ms)
Preprocessing		34	28
Feature extraction	SIFT®	227	259
	SURF®	63	54
	ORB	18	18
Feature comparison	SIFT®	6	6
	SURF®	4	4
	ORB	> 1	> 1
Total	SIFT®	317	293
	SURF®	101	86
	ORB	52	46

TABLE 5. Authentication and verification framerates.

	Feautre extraction algorithm	Xiaomi© Pocophone F1	Xiaomi© Mi 8
Authentication (FPS, 1 user)	SIFT®	3-4	4
	SURF®	6-7	7-8
	ORB	13-14	14-15
Identification (FPS, 100 user)	SIFT®	1-2 (*)	1-2 (*)
	SURF®	9-10	10
	ORB	11	11

(*) Framerate probably too low for real-time processing.

2) COMPUTING TIME PERFORMANCE

In order to obtain a real-time system for a real daily application, after analyzing the biometric performance of the software algorithms, the time invested in processing all the tasks (preprocessing, feature extraction, and feature comparison) has been measured for the TGS-CVBR® and PIS-CVBR® combination.

Fig. 14 provides the computational time of all the processes run in both devices for the UC3M-CV2 database.

The tasks are listed on the horizontal axis for each dataset and feature extraction algorithm, while the time, in seconds, spent on each task is listed on the vertical axis. The Pocophone F1 and Mi 8 datasets have been run on each device, respectively, and the full dataset (2400 images) on both smartphones. The preprocessing task has been plotted in green due to its independence to the feature extraction algorithm. This figure illustrates the fact that, for all the datasets, devices, and algorithms, the highest cost of time is in the feature or descriptor extraction and feature comparison (intraclass and interclass comparison). Also, it is remarkable that SIFT® is the slowest algorithm, and ORB is the fastest, as should be expected from their evidenced track record. Table 4, reinforces this fact, summarizing the unit processing values for each device. As was

mentioned in 3) TGS-CVBR® and PIS-CVBR® combined: decision policy section and to test the real influence of these facts, the authentication/verification, and identification processes have been shown in real-time on the devices' screen.

Table 5 shows the framerate, in Frames Per Second (FPS), for each feature extraction algorithm and its corresponding feature comparison algorithm. The FPS rate, shown in the identification row, evidences a higher computational cost in identification than in authentication (comparison of 1 user against comparison of 100 users). The table illustrates, as expected, that SIFT® (FLANN matching) provides the slowest FPS rate, but 3-4 FPS and 1-2 FPS are probably enough, depending on the final application, to authenticate (1 user) and identify (100 users), respectively. The rates for the three algorithms are higher for the Mi 8 device, showing for this device a faster processing performance. This fact is in concordance with the smaller unit processing values obtained (Table 4) on the Mi 8 device.

IV. CONCLUSION

In this paper, a novel contactless vascular biometric recognition system for wrist vein modality has been created, tested, and completely embedded into a smartphone. The non-contact interaction with the smartphone, intended for screen unlocking and more secure online payments, has been the motivation behind this work. For this purpose, the near-infrared camera, and near-infrared LED, originally integrated for facial recognition into the Xiaomi© Pocophone F1 and Xiaomi© Mi 8 devices, have been accessed. Two novel algorithms have been proposed in order to deal with the image variability due to the absence of physical contact or fixing mechanism of the wrist area:

1) *TGS-CVBR®: algorithm to guide the subject on how to place the wrist correctly during the collection of the database and the recognition process.*
2) *PIS-CVBR®: algorithm in charge of the recognition goal through the image preprocessing, feature extraction, feature comparison, and final decision task.*

To verify and test the biometric and computing time performance of these algorithms on the two mobile devices, 2400 infrared images from 50 subjects (100 wrists) have been collected in a contactless way (UC3M-CV2 database).

The results have been focused on the employed feature or keypoint extraction algorithms: SIFT®, SURF®, and ORB. The biometric performance analysis shows that the SIFT® algorithm provides the best recognition results. The EER obtained fluctuates between 6,82 % (best case, Session 2 on Mi 8 device) and 18,72 % (worst case, full UC3M-CV2). As a first approach, using a smartphone camera in a non-physical-contact way, these values are promising in order to integrate this technology with the rest of the existing biometric systems on smartphones. This work provides a low-cost solution to keep improving the contactless interaction with these accessible devices. Also, it presents the possibility of easily integrating the non-contact vascular recognition into any system, with simple biometric hardware specifications.

Nevertheless, the biometric recognition values are far from being acceptable, with a marked opportunity for improvement considering, for example, the FMR values stated by Apple Inc.© in fingerprint (Touch ID, FMR = 0.002 % [39]) and facial recognition (Face ID, FMR = 0.0001 % [40]). Unfortunately, in order to compare the three biometric modalities into a smartphone, as far as is known, these values are not available for the devices used. The current State-of-the-Art of wrist VBR and trendy Deep Learning techniques (CNNs) applied in other vascular variants, also claim better biometric performance. They should be considered and compared taking into account the new scenario proposed in this paper: smartphone as a capture device, contactless acquisition, and external environmental light influence.

The computing time performance analysis reflects that current devices are prepared to process and execute in real-time these types of algorithms for authentication. The slowest one, SIFT®, only presents a probably low FPS rate for identification. This fact is acceptable considering that it is a proof of concept and that smartphones are usually used only for verification or authentication applications (e.g., online payments, bank account access, and screen unlocking), but not identification (e.g., access control and forensic applications).

For future works, all efforts will be focused on improving recognition accuracy.

REFERENCES

[1] R. Garcia-Martin and R. Sanchez-Reillo, "Wrist vascular biometric recognition using a portable contactless system," *Sensors*, vol. 20, no. 5, p. 1469, Mar. 2020.
[2] T. Endoh, T. Aoki, M. Goto, and M. Watanabe, "Individual identification device," U.S. Patent 8 190 239 B2, Jul. 7, 2005.
[3] K. Kitane, "Fingervein Authentication Unit," U.S. Patent 20 110 222 740 A1,Sep. 15, 2011.
[4] R. Raghavendra and C. Busch, "A low cost wrist vein sensor for biometric authentication," in *Proc. IEEE Int. Conf. Imag. Syst. Techn. (IST)*, Oct. 2016, pp. 201–205.
[5] J. E. S. Pascual, J. Uriarte-Antonio, R. Sanchez-Reillo, and M. G. Lorenz, "Capturing hand or wrist vein images for biometric authentication using low-cost devices," in *Proc. 6th Int. Conf. Intell. Inf. Hiding Multimedia Signal Process.*, Oct. 2010, pp. 318–322.
[6] *Vivo X20*. Accessed: Mar. 5, 2020. [Online]. Available: https://www.gsmarena.com/vivo_x20-8852.php
[7] *Huawei Mate 20 Pro*. Accessed: Mar. 5, 2020. [Online]. Available: https://consumer.huawei.com/uk/phones/mate20-pro/
[8] *Samsung Galaxy S8*. Accessed: Mar. 5, 2020. [Online]. Available: https://www.samsung.com/uk/smartphones/galaxy-s8/
[9] *Google Assistant*. Accessed: Mar. 5, 2020. [Online]. Available: https://assistant.google.com/
[10] Fernandez-Lopez, Liu-Jimenez, Kiyokawa, and Wu, "Recurrent neural network for inertial gait user recognition in smartphones," *Sensors*, vol. 19, no. 18, p. 4054, Sep. 2019.
[11] M. J. Coakley, J. V. Monaco, and C. C. Tappert, "Keystroke biometric studies with short numeric input on smartphones," in *Proc. IEEE 8th Int. Conf. Biometrics Theory, Appl. Syst. (BTAS)*, Sep. 2016, pp. 1–6.
[12] T. Kutzner, F. Ye, I. Bonninger, C. Travieso, M. Kishore Dutta, and A. Singh, "User verification using safe handwritten passwords on smartphones," in *Proc. 8th Int. Conf. Contemp. Comput. (IC)*, Aug. 2015, pp. 48–53.
[13] *LG G8 ThinQ (hand ID)*. Accessed: Mar. 5, 2020. [Online]. Available: https://www.lg.com/uk/mobile-phones/lg-LMG810EAW
[14] C. Mohamed, Z. Akhtar, B. N. Eddine, and T. H. Falk, "Combining left and right wrist vein images for personal verification," in *Proc. 7th Int. Conf. Image Process. Theory, Tools Appl. (IPTA)*, Nov. 2017, pp. 1–6.

[15] L. Debiasi, C. Kauba, B. Prommegger, and A. Uhl, "Near-infrared illumination add-on for mobile hand-vein acquisition," in *Proc. IEEE 9th Int. Conf. Biometrics Theory, Appl. Syst. (BTAS)*, Oct. 2018, pp. 1–9.
[16] I. Patil, S. Bhilare, and V. Kanhangad, "Assessing vulnerability of dorsal hand-vein verification system to spoofing attacks using smartphone camera," in *Proc. IEEE Int. Conf. Identity, Secur. Behav. Anal. (ISBA)*, Feb. 2016, pp. 1–6.
[17] R. S. Kuzu, E. Piciucco, E. Maiorana, and P. Campisi, "On-the-fly finger-vein-based biometric recognition using deep neural Networks," *IEEE Trans. Inf. Forensics Security*, vol. 15, pp. 2641–2654, 2020.
[18] R. Kabacinski and K. Kowalski, "Vein pattern database and benchmark results," *Electron. Lett.*, vol. 47, no. 20, pp. 1127–1128, 2011.
[19] L. Wang, G. Leedham, and S.-Y. Cho, "Infrared imaging of hand vein patterns for biometric purposes," *IET Comput. Vis.*, vol. 1, no. 3, pp. 113–122, Dec. 2007.
[20] J. Uriarte-Antonio, D. Hartung, J. E. S. Pascual, and R. Sanchez-Reillo, "Vascular biometrics based on a minutiae extraction approach," in *Proc. Carnahan Conf. Secur. Technol.*, Oct. 2011, pp. 1–7.
[21] A. Das, U. Pal, M. A. F. Ballester, and M. Blumenstein, "A new wrist vein biometric system," in *Proc. IEEE Symp. Comput. Intell. Biometrics Identity Manage. (CIBIM)*, Dec. 2014, pp. 68–75.
[22] O. Nikisins, T. Eglitis, A. Anjos, and S. Marcel, "Fast cross-correlation based wrist vein recognition algorithm with rotation and translation compensation," in *Proc. Int. Workshop Biometrics Forensics (IWBF)*, Jun. 2018, pp. 1–7.
[23] Y. Matsuda, N. Miura, A. Nagasaka, H. Kiyomizu, and T. Miyatake, "Finger-vein authentication based on deformation-tolerant feature-point matching," *Mach. Vis. Appl.*, vol. 27, no. 2, pp. 237–250, Feb. 2016.
[24] C. Harris and M. Stephens, "A combined corner and edge detector," in *Proc. Alvey Vis. Conf.*, 1988, pp. 1–5.
[25] R. Das, E. Piciucco, E. Maiorana, and P. Campisi, "Convolutional neural network for Finger-Vein-Based biometric identification," *IEEE Trans. Inf. Forensics Security*, vol. 14, no. 2, pp. 360–373, Feb. 2019.
[26] J. M. Song, W. Kim, and K. R. Park, "Finger-vein recognition based on deep DenseNet using composite image," *IEEE Access*, vol. 7, pp. 66845–66863, 2019.
[27] A. Uhl, C. Busch, S. Marcel, and R. Veldhuis, *Handbook of Vascular Biometric*. Cham, Switzerland: Springer, 2020.
[28] R. Garcia-Martin and R. Sanchez-Reillo. *Vein Biometric Recognition on a Smartphone*. Accessed: May 12, 2020. [Online]. Available: https://joinup.ec.europa.eu/solution/vein-biometric-recognition-smartpho-neFile:Vein_Biometric_Recognition_on_a_Smartphone-Python_Code_V1.0.py
[29] *Information Technology—Biometric Performance Testing and reporting—Part 1: Principles and Framework*, Standard ISO/IEC 19795-1, American National Standards Institute, May 2019,
[30] *Xiaomi Pocophone F1*. Accessed: Mar. 5, 2020. [Online]. Available: https://www.mi.com/uk/pocophone-f1/
[31] *Xiaomi Mi 8*. . Accessed: Mar. 5, 2020. [Online]. Available: https://www.mi.com/uk/mi8/
[32] S. M. Pizer, E. P. Amburn, and J. D. Austin, "Adaptive histogram equalization and its variations," *Comput. Vis., Graph., Image Process.*, vol. 39, pp. 355–368, Sep. 1987.
[33] D. G. Lowe, *Distinctive Image Features from Scale-Invariant Keypoints*. Vancouver, BC, Canada: Univ. British Columbia, Jan. 2004.
[34] H. Bay, T. Tuytelaars, and L. Gool, "SURF: Speeded up robust features," in *Proc. 9th Eur. Conf. Comput. Vis.*, Graz, Austria, 2006, pp. 404–417.
[35] E. Rublee, V. Rabaud, K. Konolige, and G. Bradski, "ORB: An efficient alternative to SIFT or SURF," in *Proc. Int. Conf. Comput. Vis.*, Nov. 2011, pp. 2564–2571.
[36] P. F. Clotet and R. D. Findling, "Mobile wrist vein authentication using SIFT features," in *Computer Aided Systems Theory—EUROCAST*. Cham, Switzerland: Springer, 2017. [Online]. Available: https://link.springer.com/chapter/10.1007/978-3-319-74718-7_25
[37] M. Muja and D. G. Lowe, "FLANN—Fast library for approximate nearest neighbor user manual," in *Proc. Int. Conf. Comput. Vis. Theory Appl. (VISAPP)*, Jan. 2013, pp. 1–29.
[38] *The General Data Protection Regulation (GDPR)*, document Regulation (EU) 02016R0679 of the European Parliament and of the Council of, Apr. 2016.
[39] (Sep. 2017). *About Touch ID Advanced Security Technology*. Apple Inc. Accessed: Mar. 5, 2020. [Online]. Available: https://support.apple.com/en-us/HT204587
[40] (Feb. 2020). *About Face ID Advanced Technology*. Apple Inc. Accessed: Mar. 5, 2020. [Online]. Available: https://support.apple.com/en-us/HT208108

RAUL GARCIA-MARTIN received the bachelor's degree in industrial electronics and automation engineering and the master's degree in electronics systems and applications engineering from the University Carlos III of Madrid (UC3M), in 2016 and 2018, respectively, where he is currently pursuing the Ph.D. degree with the University Group for Identification Technologies (GUTI), researching on vascular biometric recognition. At the same time, he acquired experience in industrial applications as a Software and Hardware Developer in several companies.

RAUL SANCHEZ-REILLO (Senior Member, IEEE) received the Ph.D. degree in telecommunication engineering from the Universidad Politecnica de Madrid, in 2000. He is currently a Full Professor with the University Carlos III of Madrid (UC3M). He is also the Head of the University Group for Identification Technologies (GUTI). His Research and Development Group is involved in project development related to identification technologies, either by the user of secure elements (such as smartcards) and/or by using biometrics. In addition to research and development activities, he has also managed projects concerning a broad range of applications, from Social Security Services till Financial Payment Methods. He has taken part in European Projects, being the WP Leader in most of them. He is a member of SC17, SC27, and SC37 Standardization Committees, holding the international secretary of SC17 WG11 and SC37 WG2. In 2009, he founded the IDTestingLab, an evaluation laboratory for identification products.